Journal of Organometallic Chemistry 857 (2018) 145–151

Contents lists available at ScienceDirect

Journal of Organometallic Chemistry

journal homepage: www.elsevier.com/locate/jorganchem

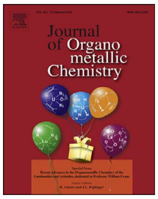

Dispersion and distortion in heavy group 2 and lanthanide decamethylmetallocenes: The $(C_5Me_5)_2(Sr,Sm)$ connection☆

Ross F. Koby, Timothy P. Hanusa*

Department of Chemistry, Vanderbilt University, Nashville, TN 37235, USA

A R T I C L E I N F O

Article history:
Received 16 August 2017
Received in revised form
7 November 2017
Accepted 8 November 2017
Available online 10 November 2017

Keywords:
Density functional theory
Dispersion
Metallocenes
Samarium
Strontium

A B S T R A C T

Identification of the source(s) of the counterintuitive bending (non-linearity) in heavy group 2 (Ca–Ba) dihalides and metallocenes has long been in dispute, a difficulty compounded by the low values of energy involved (ca. $\lesssim$ 2 kcal mol^{-1}). Analogous issues exist with compounds of the divalent lanthanides Sm(II), Eu(II), and Yb(II), despite the substantially different electronic structures of the metals involved. The assertion that the bent structure of $(C_5Me_5)_2Sr$, for example, can be attributed exclusively to the operation of attractive dispersion forces between the ring methyl groups has been argued on the basis of molecular mechanics calculations, and more recently with the aid of DFT studies that employed dispersion-corrected density functionals (Organometallics, 32(5) (2012), 1265). In contrast, covalent interactions have been identified as the primary source of bending in the similarly distorted $(C_5Me_5)_2Sm$. The case of bent $(C_5Me_5)_2Sr$ has been reinvestigated with the use of larger basis sets for strontium, and with the employment of the "dispersion-free" APF density functional. We find that given flexible enough basis sets, bending can be modeled even in the absence of explicitly included dispersion effects, and that both inherent electronic effects and dispersion interactions contribute to the bending of $(C_5Me_5)_2Sr$.

1. Introduction

The highly electropositive lanthanide (Ln) metals and the related heavy group 2 (Ae) elements calcium, strontium, and barium are characterized by metal–ligand (Ln–L or Ae–L) interactions that are strongly polar. Lacking metal valence electrons (or in the case of the lanthanides, possessing "core-like" 4f valence electrons) that could influence the orientation of ligands, a simple electrostatic analysis of the bonding in LnL_2 or AeL_2 compounds predicts that their geometries should be linear, and that LnL_3 or $[AeL_3]^-$ species should be trigonal planar, i.e., that the ligands should be as far from each other as is possible [1]. Nevertheless, it has long been known, for example, that heavy Ae difluorides (Ae = Ca–Ba) are bent in the gas phase [2], that the f-element $Ln[N(SiMe_3)_2]_3$ complexes are pyramidal [3,4], and that, with the exception of species with extremely bulky rings [5–9], almost all Cp'_2Ae complexes [10,11] (and the comparable organolanthanide metallocenes Cp'_2Sm, Cp'_2Eu, and Cp'_2Yb) [12,13] possess non-parallel cyclopentadienyl rings (Fig. 1, for the case of Cp' = C_5Me_5).

Reconciliation of an electrostatically-based bonding scheme for AeL_2 or LnL_2 compounds with their nonlinear structures has proven to be difficult, especially as the molecules are geometrically floppy (in some cases, "quasilinear") [14], with the energy required to bend the bonds from linearity or planarity to the observed values generally no more than 2 kcal mol^{-1}. Such small values can challenge computational accuracy with heavy metal compounds [2]. It is not surprising, therefore, that a range of explanations (not necessarily mutually exclusive) [15] have been proposed for the phenomena, including: 1) reverse (core) polarization of the metal cation by the ligands, i.e., perturbation of the core electrons by the ligands that induces a dipole moment, resulting in a non-uniform distribution of electrons to counteract it [1,16]; 2) for the group 2 elements, participation of $(n-1)d$ orbitals of the metal cation; 3) pseudo-Jahn Teller effect-induced distortions [17]; and 4) in appropriate complexes, attractive van der Waals (dispersion) interactions between the ligands [18]. The latter has been proposed as an explanation for the bending in the decamethylmetallocenes of Ca–Ba and Sm, Eu, and Yb, and has been supported with the use of molecular mechanics calculations that reproduce the bending angles (ring centroid–metal–ring centroid) angles observed in the

---

☆ Dedicated to Prof. William J. Evans, a mentor and friend, on the occasion of his 70th birthday.

* Corresponding author.
E-mail address: t.hanusa@vanderbilt.edu (T.P. Hanusa).

https://doi.org/10.1016/j.jorganchem.2017.11.007
0022-328X/© 2017 Elsevier B.V. All rights reserved.

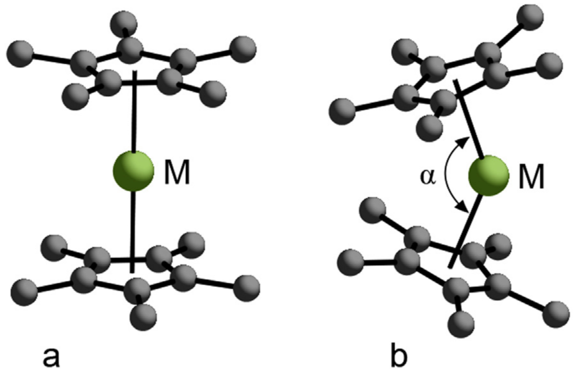

Fig. 1. Geometries of bis(pentamethylcyclopentadienyl)metal complexes: (a) parallel rings; (b) nonparallel rings (bent metallocene); α is the ring centroid–metal–ring centroid angle.

gas-phase structures [19,20]. Intriguingly, this explanation was considered but then rejected for the bending in $(C_5Me_5)_2Yb$ and $(C_5Me_5)_2No$ [21]. The reason was that the dispersion force explanation implies that the existence of the metal is irrelevant to the bent geometries. In a density functional theory (DFT) study, two $[C_5Me_5]^-$ rings sandwiching a dummy atom were found to prefer a linear (parallel ring) orientation, contrary to the result expected from the operation of interligand van der Waals attractions [21].

The potential role of dispersion interactions in the bending of Group 2 and lanthanide metallocenes has been explored more recently for the particular cases of $(C_5Me_5)_2Sr$ and $(C_5Me_5)_2Sm$ [22], especially as computational disentanglement of the explanations for bending has become feasible with the development of density functionals with additive empirical terms that capture the effects of dispersion interactions [23]. Such functionals allow dispersion corrections to be turned "on" or "off", and thus provide a means to distinguish between various bending forces in the molecules.

We have had a long-standing interest in compounds of the group 2 elements and the lanthanides, and in particular with issues of bonding and geometry for which unique explanations are not always evident. In some cases, this may take the form of structural resemblances between compounds that have no obvious reason to be similar, e.g., the comparable bending angles in stannocenes (Cp'_2Sn) and calcocenes (Cp'_2Ca), even though the former have a metal-centered lone pair of electrons that is usually cited as being responsible for the bending, and the latter do not [24]. In other cases, interligand steric effects from bulky ligands can force distortions on molecular geometries, thereby obscuring other metal-ligand interactions. Thus the structural anomalies found in various $M(E(SiMe_3)_2)_3$ complexes (M = f-element; E = N, CH) can be reproduced in calculations using orbital-free molecular mechanics methods, even though agostic M⋯(CH) interactions are also present that could produce similar effects [3].

We wondered whether a related situation existed with the group 2 metallocenes, i.e., whether the fact that molecular mechanics calculations or the use dispersion-corrected functionals reproduced the bending in the complexes might have masked other influences on their bonding. We therefore reexamined the computed geometry of $(C_5Me_5)_2Sr$, and compared it to that of $(C_5Me_5)_2Sm$. As Nief, et al., has noted [22], these two metallocenes provide a convenient pair for evaluation, as the ionic radii of Sr^{2+} and Sm^{2+} are nearly identical (1.18 Å and 1.17 Å, respectively) [25], even though the electronic structures of the ions are markedly different ([Kr] and $[Xe]4f^6$, respectively).

2. Methods

2.1. Basis set requirements

The electronic structures of the group 2 elements and their common ions ($[NG]ns^2$ and $[NG]^{2+}$, respectively) create distinctive challenges for their computational chemistry [26]. In particular, there is poor spatial separation between the valence *ns* and subvalent ("semi-core", (*n*-1)s,p) orbitals in these metals [15]. Consequently, polarization of either the valence or subvalent orbitals will influence the other, and semi-core electrons must be explicitly described in the metal basis sets used for calculations to yield calculations with meaningful results (if a pseudopotential (ECP) is used to replace some of the inner electrons, it must be "small core") [27]. Another consequence is that in the heavier group 2 metals, particular care must be used in construction of the (*n*-1)d orbitals [28], as they are formally unoccupied but have been considered "virtual states of the core" [29].

In the design of basis sets for Sr, in particular, several features must be considered. One is relativistic effects, potentially a concern in a 4th row metal such as strontium. Sadlej has argued that although relativistic effects are important in accurate polarizability calculations with the neutral Sr atom, and to a lesser extent, with the Sr^+ cation, they become "negligible" compared to electron correlation effects in the Sr^{2+} cation [30]. The small effect of relativistic corrections for calculations on molecular strontium species has been noted as well [31]. Nevertheless, relativistically corrected basis sets, either all-electron or containing ECPs that replace some of the core electrons, are available that can account for major scalar effects.

In view of the overlap between semi-core, valence, and (*n*-1) d orbitals of the group 2 metals, highly flexible valence functions must be present in the basis sets for accurate results with strontium compounds [14]. In studies of the quasilinear molecule $SrCl_2$, for example, it was shown that the use of the standard small-core Stuttgart/Dresden SDD basis set for Sr [32], which is constructed around a pseudopotential and is accompanied by a valence basis set with a 3,2 contraction of the "d" space ((6s,6p,5d) → [4s,4p,2d]), led to a linear molecule at the RHF level of theory [28]. Simply uncontracting the d shell allowed the molecule to bend (167.3°), although higher levels of theory and further elaboration of the valence basis set, including the addition of f functions, was necessary to model the experimentally determined bent structure adequately [14].

Basis sets for Sr with more flexible valence spaces than the standard one originally developed for the SDD ECP are now available, and were used in the present study. Among them are the "dhf-" segmented contracted basis sets of Weigend and Baldes [33]. These are available in split (double zeta) valence to quadruple zeta valence quality, which allows for a systematic exploration of the effect of the basis set size on the resultant geometries. The valence sets are matched with a small-core, ten-valence electron energy-consistent pseudopotential, which includes corrections for scalar relativistic effects [34]. The pseudopotential is an updated version of the original SDD ECP.

2.2. Density functional requirements

The development of density functionals designed to model dispersion interactions accurately has been one of the most actively developed areas of recent computational design, and the various approaches taken to address the issue have been reviewed [23]. For the present study, we were particularly interested in the use of specifically designed "dispersion-free" functionals, and their dispersion-corrected forms [35–37]. The rationale behind their development is not only that commonly used functionals do not describe long-range dispersion interactions correctly (e.g., with R^{-6} dependence on the interatomic distance R), but they may also display non-physical attractive or repulsive interactions that vary with R. This anomaly occurs with many commonly used functionals, including B3LYP, B3PW91, TPSS, PBE1PBE, M06-2X, and B2PLYP (Fig. 2). Empirical semiclassical corrections that patch conventional functionals (e.g., with the DFT-D*n* approach) do not correct the underlying over/underbinding, and in some cases, can worsen it [38,39].

The dispersion-free functional used in this study is APF, an empirical combination of the well-established B3PW91 and PBE1PBE functionals (with approximately 23% HF admixture) that is designed to minimize spurious dispersion interactions. The APF-D modification has a spherical atomic model for dispersion forces [37]. APF-D approximates dispersion forces with an accuracy comparable to the CCSD(T)/aug-cc-PVTZ level of theory, and its modeling of electron density is also among the very best provided by current density functionals. It provides results similar to those from *ab initio* methods such as CCSD(T) or MP2 [40].

2.3. Computational details

All geometry optimizations and energy calculations were performed with the Gaussian 09 suite of programs [41]. The majority of calculations employed the APF or APF-D functionals, described above [37]. The dhf-ECP basis sets were used for Sr [33,34]. For Sm, the small core Stuttgart-Dresden relativistic effective core potential (SDD) was used, along with its standard valence set ((12s,11p,9d,8f)/[5s,5p,4d,3f]). For comparison, the Stuttgart ECP ANO valence basis set for Sm was also tested [42]. For C and H, the def2-SVP basis sets were generally used; trial calculations with other basis sets of polarized double zeta or better quality indicated that there were only small effects on the geometry. An ultrafine integration grid (99,590) was used during all geometry optimizations, which were conducted without imposed symmetry. Based on the final structures obtained when the starting geometries were changed, the error in the calculated centroid-metal-centroid angles in the metallocenes (α) was placed at ±4°. AIM and Mulliken analyses of the molecular topology were conducted with the Multiwfn package (v. 3.3.9) [43].

3. Results and discussion

3.1. Calibration calculations

Several calculations were performed to establish the reliability of the basis sets for Sr and the APF functional to describe the geometries of the systems under investigation (Table 1). Where possible, these results were compared with experimentally determined values and various high level *ab initio* approaches.

The Sr_2 molecule in its ground state ($X^1\Sigma_g^+$) is not covalently bound, and its binding energy (1081.6 cm^{-1}, 3.09 kcal mol^{-1}) [44] is reflective of a van der Waals dimer [45]. Nevertheless, the bond length is captured about as well with the APF functional (entry 4) as with several *ab initio* techniques (entries 2,3) [37,46]. Strontium monoxide (SrO), in contrast, is more representative of a typical strontium compound, and its bond length is readily reproduced with a variety of DFT functionals, including APF (entry 9).

Molecules of greater relevance to the metallocene systems are the strontium dihalides. Strontium fluoride is known to be a bent molecule, but the actual angle is poorly determined. The results of krypton matrix isolation studies provide a value of 108° [51], but this is almost certainly strongly distorted by interaction with the krypton matrix. CCSD(T) calculations put the bending angle at 136.9°, and DFT calculations with the B3LYP functional reduce this to 128.5° (entry 15) [52]. The value from an APF/dhf-TZVP calculation is 131.1° (entry 17), in line with the B3LYP results.

The best available estimate for the equilibrium bending angle of the quasilinear molecule $SrCl_2$ is from electron diffraction measurements coupled with corrections for anharmonic vibrations [14]. This is a difficult value to reproduce computationally (see a full

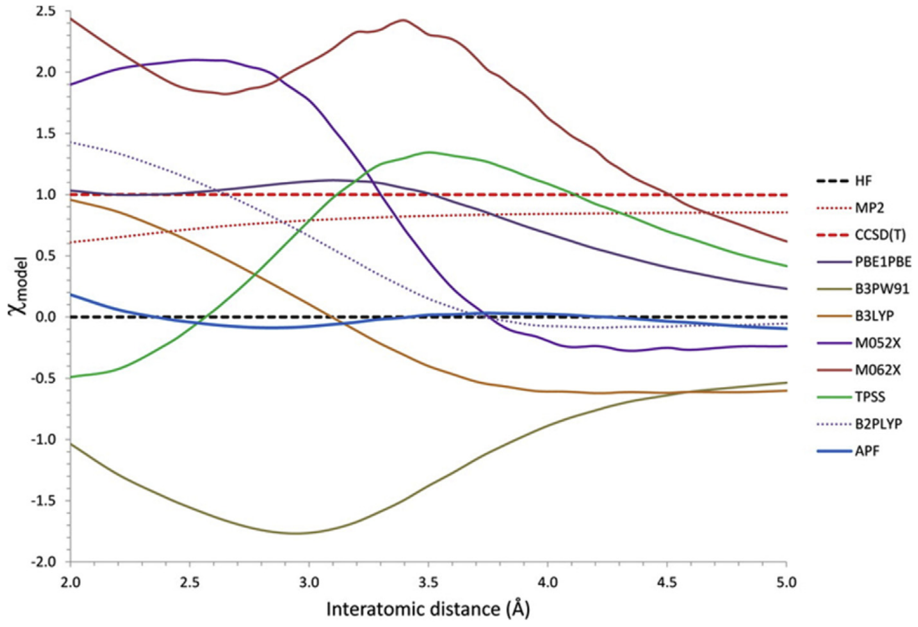

Fig. 2. Plot of $\chi(R)$, the relative error in the dispersion energy, as defined in Ref. [37] for the case of Ne_2. $\chi(R)$ will approach a constant value at long interatomic distances with a functional that includes the proper R^{-6} dependence for dispersion. Standard DFT functionals produce $\chi(R)$ that goes to 0, either from above (attractive interactions at shorter R) or from below (repulsive interactions at shorter R). APF provides minimal error in this regard. Reprinted with permission from A. Austin, G.A. Petersson, M.J. Frisch, F.J. Dobek, G. Scalmani, K. Throssell, J. Chem. Theory Comp., 8(12) (2012), 4989–5007. Copyright 2012 American Chemical Society.

Table 1
Calculated geometries of Sr_2, SrO, and strontium halides.

Entry	Complex	Method	Sr basis set	other basis	Sr–X (Å)	Angle (°)	ref.
1	Sr_2	exper. (gas phase)		n/a	4.6720(1)	n/a	[44]
2	Sr_2	CCSD(T)	CBS (extrap.)	n/a	4.710	n/a	[47]
3	Sr_2	CASPT2	ANO–RCC	n/a	4.772	n/a	[48]
4	Sr_2	APF	dhf-TZVP	n/a	4.633	n/a	a
5	Sr_2	B3LYP	dhk-TZVP	n/a	4.827	n/a	a
6	Sr_2	M06	dhk-TZVP	n/a	4.532	n/a	a
7	SrO	exper. (gas phase)			1.9199	n/a	[49]
8	SrO	CISD	Sadlej pVTZ	cc-pVTZ	1.917	n/a	[50]
9	SrO	APF	dhk-TZVP	def2-TZVP	1.907	n/a	a
10	SrO	B3LYP	dhk-TZVP	def2-TZVP	1.929	n/a	a
11	SrO	M06	dhk-TZVP	def2-TZVP	1.901	n/a	a
12	SrF_2	exper. (Kr matrix–IR)			2.20	108	[51]
13	SrF_2	CCSD(T)	SDD(uc)+f[b]	cc-pVTZ	2.142	136.9	[17]
14	SrF_2	CISD	SDD(uc)+f[b]	SDD	2.161	138.8	[28]
15	SrF_2	B3LYP	SDD(uc)+f[b]	cc-pVTZ	2.119	128.5	[52]
16	SrF_2	APF	SDD	def2-TZVP	2.124	130.6	a
17	SrF_2	APF	dhf-TZVP	def2-TZVP	2.115	131.1	a
18	$SrCl_2$	exper. (ED, equil. values)			2.607(13)	143.3(3.4)	[14]
19	$SrCl_2$	CCSD(T)	SDD(uc)+f[b]	cc-pVTZ	2.634	167.3	[17]
20	$SrCl_2$	CISD	SDD(uc)+f[b]	SDD	2.640	159.5	[28]
21	$SrCl_2$	B3LYP	SDD(uc)+f[b]	cc-pVTZ	2.632	155.5	[52]
22	$SrCl_2$	APF	SDD	def2-TZVP	2.612	151.6	a
23	$SrCl_2$	APF	dhf-TZVP	def2-TZVP	2.602	149.0	a

[a] This work.
[b] The valence d orbitals were uncontracted and a single f orbital was added.

discussion of the issue in ref. [14]), although the APF/dhf-TZVP combination gets within 6° of the angle (entry 23).

3.2. Calculations on $(C_5H_5)_2(Sr,Sm)$

Both $(C_5H_5)_2Sr$ and $(C_5H_5)_2Sm$ have long been known, although the structure of neither has been experimentally determined. They are presumed to be polymeric in the solid state [53,54]. The parent $(C_5H_5)_2Sr$ molecule has been studied computationally several times, and both bent [55] and linear [56–58] forms have been found as the lowest energy configuration. The energy difference between the conformations is consistently found to be small, and not surprisingly, the results are sensitive to the level of calculation employed. As an example, an early calculation reported that $(C_5H_5)_2Sr$ optimized to a bent structure ($\alpha = 145°$) with the use of the BP86 functional and DFT-optimized all-electron DGDZVP basis set [55]. We repeated the calculation with the same functional and basis set, and also found a bent geometry (Table 2, entry 1), although the angle is larger ($\alpha = 164°$), perhaps because we conducted a full optimization (no imposed symmetry) rather than a limited one (only ring rotation and the bending angle were varied in the original study). A reinvestigation of this system by the same authors [58] using a triple-ζ Slater-type orbital with a frozen core (3d and below) and the BP86 functional found that $(C_5H_5)_2Sr$ optimized to a linear structure; the previous bent structure was ascribed to deficiencies in the DGDZVP basis. Actually, issues with the functional need to be considered as well, as we find that the combination of the APF functional and the DGDZVP basis set also optimizes to a linear structure (entry 2). This suggests that it is the BP86/DGDZVP *combination* that overbinds the molecule. Several additional test calculations were then performed on $(C_5H_5)_2Sr$ to ensure that there were no spurious effects on the geometries induced by the APF(-D) functional (entries 3–5).

Table 2
Geometry of $(C_5H_5)_2M$ optimized with various functional/basis set combinations.

Entry	Complex	Functional	M basis set[a]	M–centroid (Å)	Angle (deg)
1	$(C_5H_5)_2Sr$	BP86	DGDZVP[b]	2.537	164.1
2	$(C_5H_5)_2Sr$	APF	DGDZVP[b]	2.532	180
3	$(C_5H_5)_2Sr$	APF	SDD	2.539	180
4	$(C_5H_5)_2Sr$	APF-D	SDD	2.533	180
5	$(C_5H_5)_2Sr$	APF	dhf-TZVP	2.520	180
6	$(C_5H_5)_2Sr$	B3LYP-D3	SDD[c]	2.550	180
7	$(C_5H_5)_2Sm$	APF	SDD	2.495	147.7
8	$(C_5H_5)_2Sm$	APF	ANO/ECP	2.494	141.9

[a] def2-SVP is used on C, H in all calculations using the APF(-D) functionals.
[b] the corresponding DGDZVP basis was also used on C, H.
[c] 6-31G(d,p) on C, H.

With the SDD basis set on Sr and the APF functional, a linear geometry is again obtained for $(C_5H_5)_2Sr$ (entry 3). This is the same result found with the BP86 functional and the SDD basis set on Sr [57]. Adding dispersion corrections with APF-D does not change the result (entry 4). With the larger dhf-TZVP valence set on Sr, $(C_5H_5)_2Sr$ still stays linear (entry 5). As a check with one of the functional/basis set combinations previously used to study the decamethylmetallocenes [22], $(C_5H_5)_2Sr$ also remains unbent with the B3LYP-D3/SDD combination (entry 6). With the exception of the problematic entry 1, all these DFT results support conclusions from previous CCSD(T) calculations; i.e., that to a high level of approximation, $(C_5H_5)_2Sr$ has a linear or quasilinear geometry [57].

A different situation exists with the samarium analogue, $(C_5H_5)_2Sm$; it also has been the subject of previous studies, where it is always found to be bent at levels of theory above Hartree-Fock [56,59]. With the use of the standard double-ζ valence set on the SDD ECP, $(C_5H_5)_2Sm$ bends with an angle of 147.7° (entry 7). With the use of the larger Stuttgart ANO/ECP basis set, used in a previous study of the bending angle of $(C_5Me_5)_2Sm$ [22], the bending angle of $(C_5H_5)_2Sm$ (141.9°, entry 8) is not far from that found in the crystal structure ($\alpha = 140.1°$) [12], which supports the conclusion that dispersive interactions between the methyl groups are comparatively unimportant contributors to its bending.

3.3. $(C_5Me_5)_2Sr$ calculations

The determination of how well various methods reproduce the geometry of $(C_5Me_5)_2Sr$ is tempered by the fact that its structure is known only from gas-phase electron diffraction measurements [60]. The thermal average ring centroid–Sr–centroid angle of 149° has an estimated error of ±3° [11]. In contrast to the experimental structure, and as previously found with the SDD basis set and various functionals without explicit dispersion corrections, $(C_5Me_5)_2Sr$ optimizes to a linear geometry with the APF functional (Table 3, entry 1). Addition of the SAM dispersion correction leads to a bent molecule with a centroid–Sr–centroid angle of 146.6° (entry 2). This is consistent with the values of 145–153° previously found with the SDD basis and other commonly used functionals, including B3LYP-D3, M05, M05-2X, M06, and wB97X-D [22].

Exchanging the Sr SDD basis set for the dhf-SVP + ECP basis combination replaces both the ECP and the valence functions; for the latter, the p and d functions are contracted differently, and a single f function has been added [33]. Nevertheless, $(C_5Me_5)_2Sr$ remains unbent at this level with the APF functional (entry 3). With the APF-D functional, the molecule again strongly bends ($\alpha = 147.9°$, entry 4).

Compared with the def-SVP basis for Sr, dhf-TZVP adds extra s and p functions, and supplies a different contraction pattern for the d polarization functions ((8s,8p,5d,1f) → [6s,5p,3d,1f]). With the APF functional, this change results in a very slightly bent $(C_5Me_5)_2Sr$ ($\alpha = 174.8°$, entry 5). This amount of bending is barely outside the error limit of a significant difference from 180°, but bending persisted even using tighter convergence criteria (10^{-4} au in maximum force), and we take it as real effect. Application of the dispersion correction not surprisingly led to a much more strongly bent molecule, with a centroid–Sr–centroid angle of 147.2° (entry 6).

Finally, use of the def-QZVP basis ((9s,9p,6d,2f,1g) → [7s,6p,4d,2f,1g]) with the APF functional led to an unambiguously bent molecule ($\alpha = 160.6°$, entry 7). The angle is relatively unaffected by the basis sets on C and H, as long as they are polarized double zeta or better (entries 8, 9). The bent structure is a minimum on the potential energy surface ($N_{imag} = 0$), and forcing the molecule to remain linear during optimization with imposed D_5 symmetry resulted in the generation of 2 imaginary frequencies (-23 cm^{-1}). These results indicate that bending of $(C_5Me_5)_2Sr$ is possible even with the use of a functional that is explicitly designed not to capture dispersion interactions. Using the SAM dispersion correction resulted in further bending to 146.2° (entry 10). It should be noted that the energy difference ($\Delta H°$) between the bent structure of entry 10 and that of the linear counterpart (D_5 symmetry) is only 0.51 kcal mol^{-1}, in line with other estimates of the bending force [57]. It is also a testament to the very small amounts of energy that are involved in these calculations. The results with the dhf-basis sets and APF(-D) functional are summarized in Table 3, entries 3–10, and are depicted in Fig. 3.

Table 3
Geometry of $(Me_5C_5)_2Sr$ optimized with various functional/basis set combinations.

Entry	Method	Sr basis set	C, H basis sets	Sr–centr (Å)	Angle (α, deg)
1	APF	SDD	def2-SVP	2.517	180
2	APF-D	SDD	def2-SVP	2.486	146.6
3	APF	dhf-SVP	def2-SVP	2.508	180
4	APF-D	dhf-SVP	def2-SVP	2.479	147.9
5	APF	dhf-TZVP	def2-SVP	2.502	174.8
6	APF-D	def2-TZVP	def2-SVP	2.473	147.2
7	APF	dhf-QZVP	def2-SVP	2.491	160.6
8	APF	dhf-QZVP	6-31G(d,p)	2.495	165.8
9	APF	dhf-QZVP	def2-TZVP	2.502	161.7
10	APF-D	dhf-QZVP	def2-SVP	2.467	146.2
			exper. (ED) [11]	2.469(6)	149(3)

3.4. Covalency in the bonding in $(C_5Me_5)_2Sr$

Given the low electronegativity of the heavy group 2 metals—that for Sr is ~1.0 [61]—there is no question that the bonding in their organometallic complexes, and in $(C_5Me_5)_2Sr$ in the present case, is highly polar, even if not actually electrostatic. The quantification of the polarity is difficult, as is determining how different computational treatments affect such measures. Detailed orbital analysis have been made for bonding in the group 2 metallocenes [55,57,58], and it is not the intent to repeat such information here. Rather, we wish to highlight the effect on indicators of covalency caused by the addition of methyl groups to the metallocenes, and of the use of highly flexible basis sets in the optimization of the compounds. One such indicator is the calculated charge(s) on the metal centers. Natural population charges (NPA) are relatively insensitive to basis set composition [62], and of note is that NPA charges reported for Sr in $(C_5H_5)_2Sr$ have clustered near +1.8 (i.e., +1.867 [56], +1.77 [57], +1.80 [58]), despite the use of different basis sets and computational methods. Interestingly, the NPA charge previously reported for the Sr center in $(C_5Me_5)_2Sr$, +1.53 [22], is similar to that calculated with the dhf-QZVP basis set and the APF functional, +1.60 (entry 7 Table 3). The difference in average metal charge ($\Delta q = 0.25$) between the two molecules is large enough that it likely reflects the better donor properties of the pentamethylcyclopentadienyl ring compared to the unsubstituted ligand.

An alternative investigation of the possible importance of covalent interactions was conducted with Bader's atoms in molecules (AIM) theory [63]. When examined at the B3LYP-D3/SDD level, the structure of $(C_5Me_5)_2Sr$ was found to have only three bond-critical paths between the Sr atom and the ring carbons, providing little evidence for covalence between the metal and ligands, and an additional three bond-critical paths between the methyl groups on the bent side of the molecule, taken as representing the stabilizing effect of van der Waals forces [22]. For the present study, bond-critical points and paths were calculated for $(C_5Me_5)_2Sr$ with the APF-D/dhf-QZVP optimized structure (entry 10, Table 3). Fig. 4 illustrates that bond critical paths are now clearly evident between the metal and the 10 carbon atoms in the ring, and additional ring critical points, indicative of delocalization in space, are also present. There are also three bond-critical paths found between hydrogen

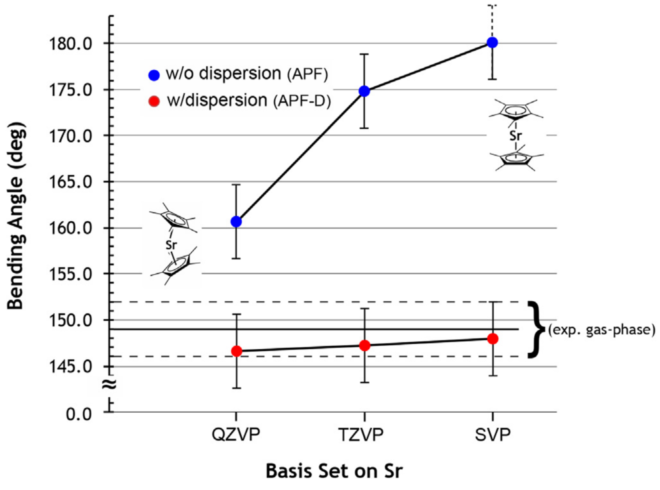

Fig. 3. Ring centroid-Sr-centroid angles for $(C_5Me_5)_2Sr$ as a function of basis set size. The dhf-basis sets are used with Sr; the def2SVP basis was used on C, H. The error bars are set at ±4°.

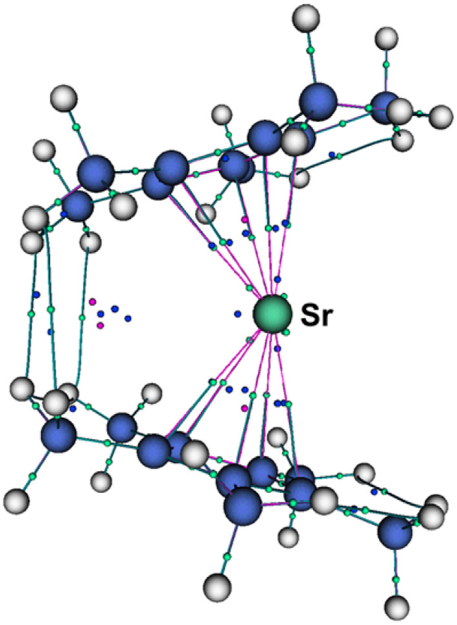

Fig. 4. AIM representation for $(C_5Me_5)_2Sr$; bond critical points are in green, ring critical points are in blue and cage critical points are in magenta. (For interpretation of the references to colour in this figure legend, the reader is referred to the web version of this article.)

atoms on the methyl groups on the bent side. The average electron density (in au) at the bond critical points along the paths from Sr to the ring carbons is 0.029, over six times the value for the points along the paths that represent van der Waals interactions between the methyl groups (avg. 0.0043). Of course, even the Sr···C interactions involve only a fraction of the electron density found in the ring bonds (e.g., the average for the bond critical paths between the ring carbons is 0.29). Nevertheless, the analysis provides evidence for both an orbital-based and a dispersion contribution to the bending.

In an analysis of the orbitals of $(C_5Me_5)_2Sm$ [22], it was noted that they fell into three different categories: one of pure metal orbitals, one of pure ligand orbitals, and one of mixed metal-ligand character (ca. 5% 4f and 10% 5d per orbital). Critically, it was also observed that the set of mixed metal-ligand orbitals was missing in $(C_5Me_5)_2Sr$, a sign of the higher ionic character in the bonding. In this context, it is noteworthy that with the dhf-QZVP basis set, evidence for mixed metal—ligand orbitals is in fact present. Fig. 5 presents the six highest occupied orbitals of $(C_5Me_5)_2Sr$. Whereas 75, 76, 79, and 80 (HOMO-5, HOMO-4, HOMO-1, and HOMO, respectively) are evidently largely ligand-based, Mulliken orbital analysis indicates that 77 (HOMO-4) contains 9.4% of Sr d character, and 78 (HOMO-2) has 7.4% d character. The mixing is not as extensive as in $(C_5Me_5)_2Sm$, but it does give an indication that the flexibility of the valence representation on the metal center can alter the calculated percentage of metal-ligand interactions.

4. Conclusions

By using the “dispersion-free” functional APF and its accompanying dispersion correction (APF-D), we have found that, provided a sufficiently flexible basis set is used on strontium, the bent structure of the heavy alkaline earth metallocene $(C_5Me_5)_2Sr$ can be shown to be bent, even without the application of dispersion corrections. However, dispersion effects do bring the bending of the metallocene into conformity with the experimentally determined structure. The methyl groups both provide the possibility for dispersion interactions and slightly increase the covalency in the metal-ring bonding, so that orbital and dispersion effects contribute together to the bending. Dispersion corrections alone can cause bending, however, and in a structurally floppy molecule such as $(C_5Me_5)_2Sr$, can mask deficiencies in the basis sets and/or density functionals used. An additional consequence of these findings is that $(C_5H_5)_2Sr$, whose linearity has been reconfirmed in this study, should not be used as a surrogate for the decamethylated species [55]. The contribution of the methyl groups to the geometry of $(C_5Me_5)_2Sr$ cannot be ignored.

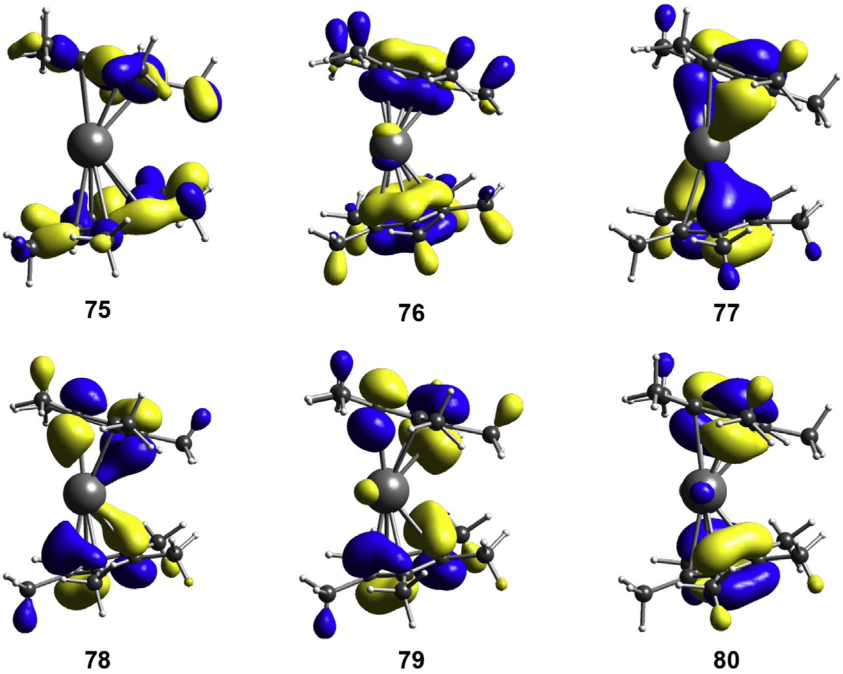

Fig. 5. Highest energy occupied orbitals of $(C_5Me_5)_2Sr$, optimized with the APF-D functional, dhf-QZVP basis set on Sr. Isodensity surfaces are drawn at the 0.40 level.

Although the covalent contribution to the bonding in $(C_5Me_5)_2Sr$ is certainly less than in the lanthanide counterpart $(C_5Me_5)_2Sm$, it is not completely negligible. These results leave the door open to orbitally based explanations of the bending, such as pseudo-Jahn Teller effect-induced distortions [17]. In this approach, mixing of excited and ground states helps supply additional covalency. The results presented here, although focused on strontium, should apply as well to calcium and barium, and to ligands other than cyclopentadienyl rings. Owing to the small energy differences involved between the geometries, future DFT studies of heavy group 2 complexes, especially those lacking chelating or other multidentate ligands that could impose a particular geometry on the molecules, will need to pay close attention to the choice of basis sets and the potentially confounding effects of density functional artifacts on the results.

Notes

The authors declare no competing financial interest.

Acknowledgment

Financial support by the National Science Foundation (CHE-1112181) and a Charles M. Lukehart Fellowship (to RFK) is gratefully acknowledged. The constructive comments of a reviewer are greatly appreciated.

References

[1] M. Guido, G. Gigli, J. Chem. Phys. 65 (1976) 1397–1402.
[2] M. Hargittai, Chem. Rev. 100 (6) (2000) 2233–2301.
[3] N.C. Boyde, S.C. Chmely, T.P. Hanusa, A.L. Rheingold, W.W. Brennessel, Inorg. Chem. 53 (18) (2014) 9703–9714.
[4] C.A.P. Goodwin, N.F. Chilton, L.S. Natrajan, M.-E. Boulon, J.W. Ziller, W.J. Evans, D.P. Mills, Inorg. Chem. 56 (10) (2017) 5959–5970.
[5] H. Sitzmann, T. Dezember, M. Ruck, Angew. Chem. Int. Ed. 37 (1998) 3114–3115.
[6] G.B. Deacon, C.M. Forsyth, F. Jaroschik, P.C. Junk, D.L. Kay, T. Maschmeyer, A.F. Masters, J. Wang, L.D. Field, Organometallics 27 (18) (2008) 4772–4778.
[7] L. Orzechowski, D.F.J. Piesik, C. Ruspic, S. Harder, Dalton Trans. 35 (2008) 4742–4746.
[8] D. Kuchenbecker, S. Harder, G. Jansen, Z. Anorg, Allg. Chem. 636 (12) (2010) 2257–2261.
[9] R.P. Kelly, T.D.M. Bell, R.P. Cox, D.P. Daniels, G.B. Deacon, F. Jaroschik, P.C. Junk, X.F. Le Goff, G. Lemercier, A. Martinez, J. Wang, D. Werner, Organometallics 34 (23) (2015) 5624–5636.
[10] R.A. Andersen, R. Blom, J.M. Boncella, C.J. Burns, H.V. Volden, Acta Chem. Scand. A41 (1987) 24–35.
[11] R.A. Andersen, R. Blom, C.J. Burns, H.V. Volden, J. Chem. Soc. Chem. Commun. (1987) 768–769.
[12] W.J. Evans, L.A. Hughes, T.P. Hanusa, R.J. Doedens, Organometallics 5 (1986) 1285–1291.
[13] R.A. Andersen, J.M. Boncella, C.J. Burns, R. Blom, A. Haaland, H.V. Volden, J. Organomet. Chem. 312 (1986) C49–C52.
[14] Z. Varga, G. Lanza, C. Minichino, M. Hargittai, Chem. – Eur. J. 12 (32) (2006) 8345–8357.
[15] M. Kaupp, Angew. Chem. Int. Ed. 40 (2001) 3534–3565.
[16] D.M. Hassett, C.J. Marsden, J. Mol. Struct. 346 (1995) 249–263.
[17] P. Garcia-Fernandez, I.B. Bersuker, J.E. Boggs, J. Phys. Chem. A 111 (41) (2007) 10409–10415.
[18] V.N. Sapunov, K. Kirchner, R. Schmid, J. Organomet. Chem. 214 (2001) 143–185.
[19] T.K. Hollis, J.K. Burdett, B. Bosnich, Organometallics 12 (1993) 3385–3386.
[20] T.V. Timofeeva, J.-H. Lii, N.L. Allinger, J. Am. Chem. Soc. 117 (1995) 7452–7459.
[21] N. Kaltsoyannis, M.R. Russo, J. Nucl. Sci. Technol. 39 (sup3) (2002) 393–399.
[22] S. Labouille, C. Clavaguéra, F. Nief, Organometallics 32 (5) (2012) 1265–1271.
[23] J. Klimeš, A. Michaelides, J. Chem. Phys. 137 (12) (2012) 120901.
[24] D.J. Burkey, T.P. Hanusa, Comments Inorg. Chem. 17 (1995) 41–77.
[25] R.D. Shannon, Acta Crystallogr. Sect. A 32 (1976) 751–767.
[26] K.G. Dyall, J. Phys. Chem. A 113 (45) (2009) 12638–12644.
[27] Y. Minenkov, G. Bistoni, C. Riplinger, A.A. Auer, F. Neese, L. Cavallo, Phys. Chem. Chem. Phys. 19 (14) (2017) 9374–9391.
[28] M. Kaupp, P.v.R. Schleyer, H. Stoll, H. Preuss, J. Am. Chem. Soc. 113 (1991) 6012–6020.
[29] L. von Szentpály, P. Schwerdtfeger, Chem. Phys. Lett. 170 (1990) 555–560.
[30] A.J. Sadlej, M. Urban, J. Mol. Struct. THEOCHEM (1991) 147–171.
[31] K.M. Fromm, E.D. Gueneau, G. Bernardinelli, H. Goesmann, J. Weber, M.J. Mayor-López, P. Boulet, H. Chermette, J. Am. Chem. Soc. 125 (12) (2003) 3593–3604.
[32] M. Kaupp, P.v.R. Schleyer, H. Stoll, H. Preuss, J. Chem. Phys. 94 (1991) 1360–1366.
[33] F. Weigend, A. Baldes, J. Chem. Phys. 133 (17) (2010) 174102.
[34] I.S. Lim, H. Stoll, P. Schwerdtfeger, J. Chem. Phys. 124 (3) (2006) 034107.
[35] K. Pernal, R. Podeszwa, K. Patkowski, K. Szalewicz, Phys. Rev. Lett. 103 (26) (2009) 263201.
[36] R. Podeszwa, K. Szalewicz, J. Chem. Phys. 136 (16) (2012) 161102.
[37] A. Austin, G.A. Petersson, M.J. Frisch, F.J. Dobek, G. Scalmani, K. Throssell, J. Chem. Theory Comp. 8 (12) (2012) 4989–5007.
[38] S. Grimme, J. Antony, S. Ehrlich, H. Krieg, J. Chem. Phys. 132 (2010), 154104/1–154104/19.
[39] S. Grimme, S. Ehrlich, L. Goerigk, J. Comput. Chem. 32 (7) (2011) 1456–1465.
[40] M.G. Medvedev, I.S. Bushmarinov, J. Sun, J.P. Perdew, K.A. Lyssenko, Science 355 (2017) 49–52.
[41] Gaussian, M.J. Frisch, G.W. Trucks, H.B. Schlegel, G.E. Scuseria, M.A. Robb, J.R. Cheeseman, G. Scalmani, V. Barone, B. Mennucci, G.A. Petersson, H. Nakatsuji, M. Caricato, X. Li, H.P. Hratchian, A.F. Izmaylov, J. Bloino, G. Zheng, J.L. Sonnenberg, M. Hada, M. Ehara, K. Toyota, R. Fukuda, J. Hasegawa, M. Ishida, T. Nakajima, Y. Honda, O. Kitao, H. Nakai, T. Vreven, J.A. Montgomery Jr., J.E. Peralta, F. Ogliaro, M. Bearpark, J.J. Heyd, E. Brothers, K.N. Kudin, V.N. Staroverov, R. Kobayashi, J. Normand, K. Raghavachari, A. Rendell, J.C. Burant, S.S. Iyengar, J. Tomasi, M. Cossi, N. Rega, N.J. Millam, M. Klene, J.E. Knox, J.B. Cross, V. Bakken, C. Adamo, J. Jaramillo, R. Gomperts, R.E. Stratmann, O. Yazyev, A.J. Austin, R. Cammi, C. Pomelli, J.W. Ochterski, R.L. Martin, K. Morokuma, V.G. Zakrzewski, G.A. Voth, P. Salvador, J.J. Dannenberg, S. Dapprich, A.D. Daniels, Ö. Farkas, J.B. Foresman, J.V. Ortiz, J. Cioslowski, D.J. Fox, Gaussian 09, Revision D.01, Gaussian, Inc., Wallingford CT, 2009, p. 2009.
[42] K.L. Schuchardt, B.T. Didier, T. Elsethagen, L. Sun, V. Gurumoorthi, J. Chase, J. Li, T.L. Windus, J. Chem. Inf. Model. 47 (3) (2007) 1045–1052.
[43] T. Lu, F. Chen, J. Comp. Chem. 33 (5) (2012) 580–592.
[44] A. Stein, H. Knöckel, E. Tiemann, Eur. Phys. J. D. 57 (2) (2010) 171–177.
[45] W. Skomorowski, F. Pawłowski, C.P. Koch, R. Moszynski, J. Chem. Phys. 136 (19) (2012) 194306.
[46] The reproduction of the equilibrium bond length in the dimer does not mean that its potential energy curve is accurately accounted for. For a discussion of this point, see I.C. Gerber, J.G. Ángyán, Chem. Phys. Lett. 416 (4) (2005) 370–375.
[47] H. Li, H. Feng, W. Sun, Y. Zhang, Q. Fan, K.A. Peterson, Y. Xie, H.F. Schaefer, Mol. Phys. 111 (14–15) (2013) 2292–2298.
[48] B.O. Roos, V. Veryazov, P.-O. Widmark, Theor. Chem. Acc. 111 (2) (2004) 345–351.
[49] M. Kaufman, L. Wharton, W. Klemperer, J. Chem. Phys. 43 (3) (1965) 943–952.
[50] R.J. Buenker, H.-P. Liebermann, J. Comput. Chem. 33 (19) (2012) 1594–1602.
[51] V. Calder, D.E. Mann, K.S. Seshadri, M. Allavena, D. White, J. Chem. Phys. 51 (5) (1969) 2093–2099.
[52] J.B. Levy, M. Hargittai, J. Phys. Chem. A 104 (9) (2000) 1950–1958.
[53] P. Jutzi, N. Burford, Chem. Rev. 99 (1999) 969–990.
[54] G.B. Deacon, D. Stellfeldt, G. Meyer, Z. Anorg, Allg. Chem. 626 (3) (2000) 623–624.
[55] A.J. Bridgeman, J. Chem. Soc. Dalton. Trans. 17 (1997) 2887–2893.
[56] M. Kaupp, P.v.R. Schleyer, M. Dolg, H. Stoll, J. Am. Chem. Soc. 114 (1992) 8202–8208.
[57] V.M. Rayón, G. Frenking, Chem. — Eur. J. 8 (20) (2002) 4693–4707.
[58] A.J. Bridgeman, C.J. Empson, Chem. — Eur. J. 12 (8) (2006) 2252–2262.
[59] K. Tatsumi, Kidorui 28 (1996) 272–273.
[60] To the best of our knowlege, the crystal structure of $(C_5Me_5)_2Sr$ has not been reported in the open literature; the Cambridge Structure Database (v. 5.38, November, 2016) has no entry for the compound. The reference cited for this in [22], which purportedly describes the solid state structure, is actually for the gas-phase structure determined by Blom, et al. (ref. [11]). Hence the values for the solid state bond distances and angles of $(C_5Me_5)_2Sr$ listed in Table 1 of [22] cannot be used as reference numbers.
[61] C.H. Suresh, N. Koga, J. Am. Chem. Soc. 124 (8) (2002) 1790–1797.
[62] A.E. Reed, R.B. Weinstock, F.J. Weinhold, J. Chem. Phys. 83 (1985) 735–746.
[63] R.F.W. Bader, Atoms in Molecules: a Quantum Theory, Oxford University Press, New York, 1994.